

Inference for interacting linear waves in ordered and random media

P. Tyagi^{1,2}, A. Pagnani^{3,4}, F. Antenucci¹, M. Ibáñez Berganza^{5,2}, L. Leuzzi^{1,2}

¹ IMIP-CNR, Rome Unit *Kerberos*, Piazzale Aldo Moro 2, 00152 - Rome, Italy

² Department of Physics, *La Sapienza* University, Piazzale Aldo Moro 2, Rome, Italy

³ Department of Applied Science and Technology and Center for Computational Sciences, Politecnico di Torino, Corso Duca degli Abruzzi 24, Torino, Italy

⁴ Human Genetics Foundation-Torino, Via Nizza 52, Torino, Italy

⁵ INFN, Gruppo Collegato di Parma, via G.P. Usberti, 7/A - 43124, Parma, Italy

Abstract. A statistical inference method is developed and tested for pairwise interacting systems whose degrees of freedom are continuous angular variables, such as planar spins in magnetic systems or wave phases in optics and acoustics. We investigate systems with both deterministic and quenched disordered couplings on two extreme topologies: complete and sparse graphs. To match further applications in optics also complex couplings and external fields are considered and general inference formulas are derived for real and imaginary parts of Hermitian coupling matrices from real and imaginary parts of complex correlation functions. The whole procedure is, eventually, tested on numerically generated correlation functions and local magnetizations by means of Monte Carlo simulations.

Classical XY spin models with linearly interacting spins have been subject of intensive study in statistical mechanics since the mid 60's concerning the investigation of critical phenomena [1]. In particular, starting as classical lattice field proxy for the quantum theory of the λ -transition of the Bose condensation of optical phonons [2], and further of liquid helium to its super fluid state [3], these models have been employed in the theoretical description of the 2D Kosterlitz-Thouless transition to an ordered unmagnetized spin vortex phase [4, 5, 6] and, more generally, to the study of the chirality transition [7, 8, 9, 10] and to the critical behavior on random graphs, whose nature depends on their spectral dimension [11, 12, 13]. Further applications can be found to the roughening transition of the interface of a crystal in equilibrium with its vapor [14] and to synchronization problems approached by means of the Kuramoto model [15, 16, 17], just to make a few examples.

Pairwise XY models can, as well, describe propagation and amplification of linear waves in open and random media, as derived, e. g., in Refs. [18, 19, 20] as a classical degradation of the quantum theory for modes with overlapping resonances. In this framework, coupling constants yield information about the interaction between localized (inner) modes with discrete frequencies and radiative (outer) modes whose frequencies take values in a continuous dominion. In presence of relevant amount of disorder, the refractive index strongly and inhomogeneously depends on the spatial coordinates of the randomly placed scatterers inside the optically active medium. In these cases, a contribution to the couplings comes from the spatial overlap between the electromagnetic fields of the inner eigenmodes, modulated by a linear, inhomogeneous, susceptibility [21, 22]. A quantitative estimate of the coupling coefficients, thus, yield fundamental information about the space localization of the modes, and about the space dependence of the optical susceptibility. Eventually, XY pairwise models can be applied to another problem concerning light propagation, that is, the optimization of the transmission matrix of complex random media [23, 24], modeled as a coupling between input and output mode phases.

In the present work we undergo the investigation of statistical inference techniques on XY models to provide a methodological theoretical frame straightforwardly applicable to the above mentioned problems with a particular focus on optics. The developed tools can be applied, as well, to any pairwise interacting model whose variables can be found in p states that can be considered as discrete values of an angle, the so-called *p -clock model* [25, 26]. Recent analysis has, indeed, shown that in the large (but not so large) p limit the XY model properties are promptly recovered for finite temperature and, further, very interesting features arise at finite small p [27, 28]. For $p = 2$, eventually, one recovers the Ising (i.e., Boolean) model for which inference studies have been carried out in Refs. [29, 30].

The paper is organized as follows: in Sec. 1, we first consider the inverse graphical problem [31] for a real valued XY model. In Sec. 2, we present the study of the generic complex amplitude model with complex valued, and possibly disordered, interaction couplings and we derive the relationship between measurable correlation functions and

theoretical mode couplings under the hypothesis of a complete graph, i.e., in the so-called fully connected mean-field limit [29] where each spin is (feebly) coupled to all the others. In Sec. 3 we, further, test the obtained inference formulas on correlations numerically generated by means of Monte Carlo simulations on different kinds of underlying interacting networks, such as complete and sparse random graphs. We present our results on the efficiency of the proposed method both in the case of ordered exchange interaction and disordered couplings. Eventually, in Sec. 4, we discuss the case where the data sets for measuring the correlation functions, from which the couplings can be inferred, are small and in Sec. 5 we draw our conclusions and outline the perspectives of our work.

1. Inference in XY model with real interaction couplings

The simplest model we are going to consider consists of XY spins $\vec{\sigma} = (\cos \phi, \sin \phi)$ with angles $\phi \in [0, 2\pi)$, pairwise real valued interaction J_{ij} between sites i and j and an external field h_i . Its Hamiltonian reads

$$\mathcal{H} = - \sum_{(ij)} J_{ij} \cos(\phi_i - \phi_j) - \sum_i h_i \cos(\phi_i) \quad (1)$$

where the set of interacting pair of sites (ij) is determined by the topology of the underlying network and J_{ij} is a symmetric matrix (the graph is undirected) whose elements can take any real value, deterministic or randomly distributed. The first focus of the present work is to derive the relationship between the two-point correlation function

$$C_{ij} = \langle \vec{\sigma}_i \cdot \vec{\sigma}_j \rangle = \langle \cos \phi_i \cos \phi_j + \sin \phi_i \sin \phi_j \rangle = \langle \cos(\phi_i - \phi_j) \rangle \quad (2)$$

and the interaction couplings J_{ij} to infer the latter for the first. In Eq. (2) the average $\langle \dots \rangle$ is the ensemble average over the equilibrium distribution. Given the set of spin-spin correlation functions from experimental data, an inverse statistical problem is setup to investigate the interaction couplings among the spins in this model. Such inverse problems have been widely studied for finding: parameters of the discrete spin models using mean field theory for complete graphs [29, 30, 32, 33], structural properties of proteins from multiple sequence alignment data, [34, 35, 36] effective local brain topologies from in-vivo neural recordings [37].

1.1. Variational free energy method approach

Although the variational free energy method for XY model is somehow standard [38], we will briefly recall it here for fixing the notations. We aim at finding the probability distribution $\rho(\phi_i)$ by introducing a Lagrange multiplier λ_i to minimize the free energy subject to probability closure constraint $\sum_i \int_0^{2\pi} d\phi_i \rho(\phi_i) = 1$. The expressions for the internal energy E , entropy S and free energy F are the following:

$$E = - \sum_{i < j} \int_0^{2\pi} \int_0^{2\pi} d\phi_i d\phi_j \rho(\phi_i) \rho(\phi_j) J_{ij} \cos(\phi_i - \phi_j)$$

$$\begin{aligned}
& - \sum_i \int_0^{2\pi} d\phi_i \rho(\phi_i) h_i \cos(\phi_i) \\
S &= - \sum_i \int_0^{2\pi} d\phi_i \rho(\phi_i) \ln \rho(\phi_i) \quad , \\
F &= E - TS - \sum_i \lambda_i \left(\int_0^{2\pi} d\phi_i \rho(\phi_i) - 1 \right) \quad (3)
\end{aligned}$$

Taking the functional derivative of the free energy functional with respect to $\rho(\phi_i)$ and setting $\delta F/\delta\rho(\phi_i) = 0$, one finds the probability distribution $\rho(\phi_i)$. Let us first define:

$$\begin{aligned}
H_i^x &= \sum_j J_{ij} \langle \cos(\phi_j) \rangle + h_i \quad , \quad H_i^y = \sum_j J_{ij} \langle \sin(\phi_j) \rangle \quad , \\
H_i &= \sqrt{(H_i^x)^2 + (H_i^y)^2} \quad , \quad \alpha_i = \arctan \frac{H_i^y}{H_i^x} \quad (4)
\end{aligned}$$

and the normalisation factor:

$$Z = \int_0^{2\pi} d\phi_i \exp(H_i \cos(\phi_i - \alpha_i)) = I_0(H_i) \quad (5)$$

where $I_0(z)$ is the modified Bessel's function of the first kind. Substituting Eqs. (4) and (5) in $\delta F/\delta\rho(\phi_i) = 0$ one obtains

$$\rho(\phi_i) = \frac{\exp(H_i \cos(\phi_i - \alpha_i))}{I_0(H_i)} \quad (6)$$

The magnetization components are, then, derived averaging $\cos(\phi_i)$ and $\sin(\phi_i)$ over the probability measure $\rho(\phi_i)$, yielding

$$m_i^x = \langle \cos(\phi_i) \rangle = \frac{I_1(H_i) \cos(\alpha_i)}{I_0(H_i)} \quad , \quad m_i^y = \langle \sin(\phi_i) \rangle = \frac{I_1(H_i) \sin(\alpha_i)}{I_0(H_i)} \quad (7)$$

where the modified Bessel's function of the first kind and their derivatives read:

$$\begin{aligned}
I_1(z) &= \int_0^{2\pi} d\phi \cos(\phi) e^{z \cos(\phi)} \quad (8) \\
I_0'(z) &= I_1(z) \quad , \quad I_1'(z) = I_0(z) - \frac{I_1(z)}{z}
\end{aligned}$$

Correlation functions are consequently computed using the linear response formulas [29], i. e., deriving magnetizations with respect to perturbations in the external fields h_k and yielding

$$\begin{aligned}
C_{ik}^x &= \frac{\delta m_i^x}{\delta h_k} = \frac{\delta}{\delta h_k} \left\{ \frac{I_1(H_i) H_i^x}{I_0(H_i) H_i} \right\} \quad (9) \\
&= \frac{H_i^x}{H_i} \left(\frac{I_1'}{I_0} - \frac{I_1^2}{I_0^2} \right) \frac{\delta H_i}{\delta h_k} + \frac{I_1}{I_0 H_i} \frac{\delta H_i^x}{\delta h_k} - \frac{H_i^x}{H_i^2} \frac{I_1}{I_0} \frac{\delta H_i}{\delta h_k} \\
&= \frac{\delta H_i^x}{\delta h_k} \left[(q_i - |m_i|^2) \frac{(H_i^x)^2}{H_i^2} + (1 - q_i^2) \frac{(H_i^y)^2}{H_i^2} \right] \\
&\quad + \frac{\delta H_i^y}{\delta h_k} \frac{H_i^x H_i^y}{H_i^2} (2q_i - |m_i|^2 - 1)
\end{aligned}$$

$$C_{ik}^y = \frac{\delta m_i^y}{\delta h_k} = \frac{\delta H_i^y}{\delta h_k} \left[(q_i - |m_i|^2) \frac{(H^y)_i^2}{H_i^2} + (1 - q_i) \frac{(H^x)_i^2}{H_i^2} \right] + \frac{\delta H_i^x}{\delta h_k} \frac{H_i^x H_i^y}{H_i^2} (2q_i - |m_i|^2 - 1) \quad (10)$$

where we make use of the following substitutions:

$$q_i \equiv \langle \cos^2(\phi_i) \rangle = 1 - \frac{I_1}{I_0 H_i}, \quad |m_i|^2 = (m_i^x)^2 + (m_i^y)^2 \quad (11)$$

$$q_i - |m_i|^2 = \frac{I_1'}{I_0} - \frac{I_1^2}{I_0^2} \quad (12)$$

We further define

$$\mu_i = \frac{m_i^y}{m_i^x} \quad (13)$$

$$\frac{H_i^x}{H_i} = \cos \alpha_i = \cos[\arctan(\mu_i)] = \sqrt{\frac{1}{1 + \mu_i^2}} \quad (14)$$

$$\frac{H_i^y}{H_i} = \sin \alpha_i = \sin[\arctan(\mu_i)] = \frac{\mu_i}{\sqrt{1 + \mu_i^2}} \quad (15)$$

$$f_1^{(i)}(q_i, m_i) = \frac{q_i - |m_i|^2 + \mu_i^2(1 - q_i)}{1 + \mu_i^2} \quad (16)$$

$$f_2^{(i)}(q_i, m_i) = \frac{(1 + \mu_i^2)(1 - q_i) + \mu_i(1 - |m_i|^2)}{1 + \mu_i^2} \quad (17)$$

$$g^{(i)}(q_i, m_i) = \sqrt{\mu_i} \frac{2q_i - |m_i|^2 - 1}{1 + \mu_i^2} \quad (18)$$

Plugging the derivatives of H_i^x and H_i^y with respect to h_k into Eqs. (9)-(10) and making use of Eqs. (11) - (18), we obtain a system equation for the correlation functions $C_{ik}^{x,y}$ and the couplings matrix J_{ik} . To be compact we adopt the operator form for expressing observables equivalent to co-ordinate form: \mathbf{J} is the couplings matrix, $\mathbf{C}^{x,y}$ the two point correlation matrices, \mathbb{I} is the $N \times N$ identity matrix and for any vector $\vec{z} = \{z_1, \dots, z_N\}$, the $N \times N$ matrix $\mathbb{I}_{\vec{z}}$ is the *diag*(\vec{z}) matrix, *i.e.* a matrix with the elements of \vec{z} on the diagonal and all other elements equal to zero. The system (9)-(10), thus, reads

$$\mathbf{C}^x = \mathbb{I}_{\vec{f}_1} [\mathbf{J}\mathbf{C}^x + \mathbb{I}] + \mathbb{I}_{\vec{g}} \mathbf{J}\mathbf{C}^y \quad (19)$$

$$\mathbf{C}^y = \mathbb{I}_{\vec{g}} [\mathbf{J}\mathbf{C}^x + \mathbb{I}] + \mathbb{I}_{\vec{f}_2} \mathbf{J}\mathbf{C}^y \quad (20)$$

Let us consider the substitutions

$$\gamma_A \equiv \mathbf{J}\mathbf{C}^x + \mathbb{I} \quad (21)$$

$$\gamma_B \equiv \mathbf{J}\mathbf{C}^y \quad (22)$$

Eqs (19) and (20) for the correlation functions can be, accordingly, rewritten as

$$\mathbf{C}^x = \mathbb{I}_{\vec{f}_1} \gamma_A + \mathbb{I}_{\vec{g}} \gamma_B \quad (23)$$

$$\mathbf{C}^y = \mathbb{I}_{\vec{g}} \gamma_A + \mathbb{I}_{\vec{f}_2} \gamma_B \quad (24)$$

To infer interaction couplings of the system we solve equations (23)-(24) in γ 's yielding

$$\gamma_A = \mathbb{I}_{\vec{k}_1} \mathbf{C}^x - \mathbb{I}_{\vec{k}_2} \mathbf{C}^y \quad (25)$$

$$\gamma_B = \mathbb{I}_{\vec{k}_3} \mathbf{C}^x - \mathbb{I}_{\vec{k}_4} \mathbf{C}^y \quad (26)$$

where

$$\vec{k}_1 = \left\{ \frac{f_2^{(i)}}{\Delta_i} \right\}, \quad \vec{k}_2 = \left\{ \frac{g^{(i)}}{\Delta_i} \right\}, \quad \vec{k}_3 = - \left\{ \frac{g^{(i)}}{\Delta_i} \right\}, \quad \vec{k}_4 = \left\{ \frac{f_1^{(i)}}{\Delta_i} \right\} \quad (27)$$

$$\Delta_i \equiv f_1^{(i)} f_2^{(i)} - (g^{(i)})^2 \quad (28)$$

We, eventually, obtain the values of \mathbf{J} by inverting Eq. (21)

$$\mathbf{J} = (\gamma_A - \mathbb{I})(\mathbf{C}^x)^{-1} \quad (29)$$

and using γ_A obtained from measured correlations and magnetizations. Substituting for J_{ij} in Eq. (4) and using Eqs. (14)-(15) we, moreover, obtain the inference formula for the external field from the inferred J 's and the measured m 's:

$$\mathbb{I}_{\vec{\mu}} \vec{h} = \mathbf{J} \vec{m}^y - \mathbb{I}_{\vec{\mu}} \mathbf{J} \vec{m}^x \quad (30)$$

1.1.1. Zero external field Considering the case at $h = 0$, Eqs. (4), (7), (11)-(18) simplify as

$$H_i^x = \sum_j J_{ij} m_j^x, \quad H_i^y = 0, \quad \alpha_i = 0, \quad H_i = H_i^x \quad (31)$$

$$m_i^x = \frac{I_1(H_i)}{I_0(H_i)}, \quad m_i^y = \mu_i = 0$$

$$f_1^{(i)} = q_i - m_i^2, \quad f_2^{(i)} = 1 - q_i, \quad g_i = 0$$

and the correlation function reduces, then, to

$$C_{ik}^x = \left. \frac{\delta m_i^x}{\delta h_k} \right|_{\vec{h}=\vec{0}} = [\langle \cos^2(\phi_i) \rangle - \langle \cos(\phi_i) \rangle^2] \left(\sum_j J_{ij} C_{jk}^x + \delta_{ik} \right) \quad (32)$$

Further, inverting Eq. (32), eventually yields:

$$\mathbf{J} = \mathbb{I}_{\vec{k}_1} - (\mathbf{C}^x)^{-1}, \quad \vec{k}_1 = \left\{ (q_i - m_i^2)^{-1} \right\} \quad (33)$$

In the above Eq. (33) of inferred J , it is worth noticing the similarity with the expression of inferred J in terms of C of the Ising model with discrete spins, see, e.g., [29, 30, 33], where $\langle \cos^2(\phi_i) \rangle = 1$.

2. Model with complex spins and couplings

In this section, the interaction coupling matrix J_{ij} is considered to be a complex matrix consisting of a real and an imaginary part as $J_{ij} = J_{ij}^R + iJ_{ij}^I$ and the external field is a complex vector $h_i = h_i^R + ih_i^I$. This model can be a proxy for the propagation and interaction of waves in optically active media, ordered or random, where electromagnetic

modes can be represented, in a properly defined base of eigenvectors, by complex numbers $a_i = A_i e^{i\phi_i}$: each mode amplitude has its own magnitude $A_i = |a_i|$ and phase angle $\phi_i = \arg(a_i)$. Indeed, the electromagnetic field can be decomposed, in the slow amplitude approximation [39], in terms of the complex amplitudes of the modes localized inside the medium

$$\mathbf{E}(\mathbf{r}, t) = \sum_{k=1}^N a_k(t) \mathbf{U}_k(\mathbf{r}) e^{i\omega_k t + \phi_k} + c.c. \quad (34)$$

where the frequencies ω_k take values on a discrete dominion and \mathbf{U}_k 's are the eigenvectors of the eigenmodes in some given basis allowing for a decomposition between inner and outer modes by means of Feshbach projectors [20]. We stress that, in cavities with non-negligible leakages or cavity-less light scattering random media, the N modes indicated in the sum are by no means a complete basis, but they are the subset made of purely localized modes amplified inside the cavity.

Such modes can be proven to display a stochastic dynamics governed by a quantum Langevin dynamics [19]. In the classical limit such evolution is proved equivalent to the master equation for the density of states [20] and in terms of complex amplitudes takes the form

$$\begin{aligned} \dot{a}_n(t) &= - \sum_m \mathcal{J}_{nm} a_m + \eta_n(t) = \frac{\partial \mathcal{H}}{\partial a_n^*} + \eta_n(t) \\ \langle \eta_n(t) \rangle &= 0, \quad \langle \eta_n^*(t) \eta_{n'}(t') \rangle \simeq 2n_{\text{th}} \delta_{nm} \delta(t - t') \end{aligned} \quad (35)$$

where, for large enough heat-bath temperature, the thermal number of photons in the classical regime is $n_{\text{th}} \propto T$ and the complex valued white noise is approximated as uncorrelated on different states [40, 41]. In general, though, we recall that non-diagonal covariances in the space mode can be non-zero for Markovian dynamics [20]. The linear non-diagonal coupling \mathcal{J}_{nm} between modes is the dumping matrix, associated to the openness of the optical cavity, due, e. g., to leakages in standard lasers [42] or to the cavity-less structure of the scattering region of the optically active material in random lasers [43, 44, 45, 21]. The total power taken by the system is a constant \mathcal{E} that, rescaling the amplitudes as $a_n \rightarrow a_n / \sqrt{\omega_n}$, can be expressed as a simple spherical constraint

$$\mathcal{E} = \epsilon N = \sum_{n=1}^N |a_n|^2 \quad (36)$$

The static properties of the above dynamics can be derived by studying the Hamiltonian

$$\mathcal{H}[\{a\}] = - \sum_{(ij)} a_i J_{ij} a_j^* - \sum_i h_i a_i^* \quad (37)$$

where J_{ij} includes the dumping \mathcal{J}_{ij} , incorporating the inner-outer modes interaction, and, possibly, also includes the spatial overlap of the eigenmodes modulated by an inhomogeneous dielectric constant. We add a complex external field h_i for generality. In the present work, we assume J_{ij} to be Hermitian, thus $J_{ij}^R = J_{ji}^R$, and $J_{ij}^I = -J_{ji}^I$.

The dynamics of mode phases changes at a much faster time scale than mode amplitudes [46]. Moreover, in presence of a large number of modes and a not too diluted interaction network, in a wide variety of systems intensity equipartition occurs among all modes, i.e., $|a_i| \simeq 1$ [47], trivially satisfying constraint (36). In particular, pairwise interacting mode systems, in any graph topology, always display intensity equipartition in all thermodynamic phases. One can thus work in the so-called *quenched amplitude* approximation, that is, amplitudes are further taken as quenched and incorporated in the J 's, yielding the Hamiltonian:

$$\begin{aligned} \mathcal{H}[\{\phi\}] = & - \sum_{(ij)} [J_{ij}^R \cos(\phi_i - \phi_j) + J_{ij}^I \sin(\phi_i - \phi_j)] \\ & - \sum_i [h_i^R \cos(\phi_i) + h_i^I \sin(\phi_i)] \end{aligned} \quad (38)$$

Though derived in terms of light modes interacting in an optical open cavity, we stress that the above Hamiltonian generically describes any linear wave system. Indeed, it can, e. g., describe a class of optimization problems where the variable ϕ represents the phase of a pixel of the incoming/outcoming light propagating through a random medium, including disordered optical fibers, and J_{ij} represents the transmission matrix [23, 24].

The same variational procedure of Sec. 1 is applied to the complex system modeled by Eq. (38). The following substitutions for H_i^x and H_i^y are considered, in place of Eq. (4), in order to calculate the probability distribution $\rho(\phi_i)$:

$$H_i^x = \sum_j J_{ij}^R \langle \cos(\phi_j) \rangle - \sum_j J_{ij}^I \langle \sin(\phi_j) \rangle + h_i^R \quad (39)$$

$$H_i^y = \sum_j J_{ij}^R \langle \sin(\phi_j) \rangle + \sum_j J_{ij}^I \langle \cos(\phi_j) \rangle + h_i^I \quad (40)$$

It is found that the structure of $\rho(\phi_i)$ remains the same as in the case of real-valued J 's, cf. Eq. (6), though the components H_i^x , H_i^y and H_i adorn different expressions.

2.1. Correlation functions and inference formulas

In this section, equations for the correlation functions are derived. In the presence of complex fields, four correlation functions are found from the differentiation of magnetizations with respect to both components of the fields externally acting on the system. Using the expressions of H_i^x/H_i and H_i^y/H_i as in eqs. (14)-(15), magnetizations in Eq. (7) can be written in the following form,

$$m_i^x = \frac{I_1(H_i)}{I_0(H_i)} \frac{H_i^x}{H_i}, \quad m_i^y = \frac{I_1(H_i)}{I_0(H_i)} \frac{H_i^y}{H_i} \quad (41)$$

To derive correlation functions we use the following linear response relations,

$$C_{ik}^x = \frac{\delta m_i^x}{\delta h_k^R}, \quad \tilde{C}_{ik}^x = \frac{\delta m_i^x}{\delta h_k^I}, \quad C_{ik}^y = \frac{\delta m_i^y}{\delta h_k^R}, \quad \tilde{C}_{ik}^y = \frac{\delta m_i^y}{\delta h_k^I} \quad (42)$$

Performing the above derivatives as in Sec. 1, we find equations for the correlation functions in matrix form as following

$$\mathbf{C}^x = \mathbb{I}_{\vec{f}_1} [\mathbf{J}^R \mathbf{C}^x - \mathbf{J}^I \mathbf{C}^y + \mathbb{I}] + \mathbb{I}_{\vec{g}} [\mathbf{J}^R \mathbf{C}^y + \mathbf{J}^I \mathbf{C}^x] \quad (43)$$

$$\tilde{\mathbf{C}}^x = \mathbb{I}_{\vec{f}_1} [\mathbf{J}^R \tilde{\mathbf{C}}^x - \mathbf{J}^I \tilde{\mathbf{C}}^y] + \mathbb{I}_{\vec{g}} [\mathbf{J}^R \tilde{\mathbf{C}}^y + \mathbf{J}^I \tilde{\mathbf{C}}^x + \mathbb{I}] \quad (44)$$

$$\mathbf{C}^y = \mathbb{I}_{\vec{g}} [\mathbf{J}^R \mathbf{C}^x - \mathbf{J}^I \mathbf{C}^y + \mathbb{I}] + \mathbb{I}_{\vec{f}_2} [\mathbf{J}^R \mathbf{C}^y + \mathbf{J}^I \mathbf{C}^x] \quad (45)$$

$$\tilde{\mathbf{C}}^y = \mathbb{I}_{\vec{g}} [\mathbf{J}^R \tilde{\mathbf{C}}^x - \mathbf{J}^I \tilde{\mathbf{C}}^y] + \mathbb{I}_{\vec{f}_2} [\mathbf{J}^R \tilde{\mathbf{C}}^y + \mathbf{J}^I \tilde{\mathbf{C}}^x + \mathbb{I}] \quad (46)$$

These are decoupled two-by-two and the two subsystems are not independent, but equivalent to each other. Therefore, to obtain the inference formulas for \mathbf{J} we can simply solve Eqs. (43) and (45). To invert them let us first define:

$$\Gamma_A \equiv \mathbf{J}^R \mathbf{C}^x - \mathbf{J}^I \mathbf{C}^y + \mathbb{I} \quad (47)$$

$$\Gamma_B \equiv \mathbf{J}^R \mathbf{C}^y + \mathbf{J}^I \mathbf{C}^x \quad (48)$$

Substituting into eqs. (43), (45) and solving for Γ 's we obtain

$$\Gamma_A = \mathbb{I}_{\vec{k}_1} \mathbf{C}^x - \mathbb{I}_{\vec{k}_2} \mathbf{C}^y \quad (49)$$

$$\Gamma_B = \mathbb{I}_{\vec{k}_3} \mathbf{C}^x - \mathbb{I}_{\vec{k}_4} \mathbf{C}^y \quad (50)$$

where coefficients $\mathbb{I}_{\vec{k}_a}$ are given in Eq. (27). Now, after obtaining Γ_A and Γ_B in terms of measurable quantities, we get back to eqs. (47) and (48) and solve them to extract interaction couplings, yielding the main equations of our work:

$$\mathbf{J}^R = [(\Gamma_A - \mathbb{I})(\mathbf{C}^y)^{-1} + \Gamma_B(\mathbf{C}^x)^{-1}] [\mathbf{C}^x(\mathbf{C}^y)^{-1} + \mathbf{C}^y(\mathbf{C}^x)^{-1}]^{-1} \quad (51)$$

$$\mathbf{J}^I = [- (\Gamma_A + \mathbb{I})(\mathbf{C}^x)^{-1} + \Gamma_B(\mathbf{C}^y)^{-1}] [\mathbf{C}^x(\mathbf{C}^y)^{-1} + \mathbf{C}^y(\mathbf{C}^x)^{-1}]^{-1} \quad (52)$$

Eventually, to infer the external field values from the inferred \mathbf{J} values and the measured magnetizations, using $H_i^x = H_i^y / \mu_i$ in Eqs. (39)-(40), we obtain

$$\mathbb{I}_{\vec{\mu}} \vec{h}^R - \vec{h}^I = (\vec{n}^x + \mathbb{I}_{\vec{\mu}} \vec{n}^y) \mathbf{J}^I \quad (53)$$

3. Numerical tests

To verify the efficiency of the predictions of the inference method derived above, we present our tests on data provided by means of Monte Carlo simulations of models exactly given by Eqs. (1) and (38) with known couplings and fields and defined on different topologies.

We will first consider data generated from finite size models on fully connected long-range models, where each spin is connected to all the others and each coupling J_{ij} is vanishingly small to guarantee thermodynamic convergence. These are the hypothesis at the ground of the variational approach followed in deriving Eqs. (51-52). We will consider both the case of ordered $J_{ij} = J$ and randomly distributed J_{ij} with Gaussian probability of mean zero and variance one.

We will afterwards consider data generated on models defined on Erdos-Renyi (ER) sparse graphs [48] where the connectivity is randomly distributed according to the Poisson Distribution

$$P(k) = \frac{e^{-c} c^k}{k!} \quad (54)$$

Once again, both deterministic and quenched disordered interaction couplings are considered.

The values of the inferred matrix are, eventually, compared to those of the original matrix. All the data, namely, correlation functions C^X, C^Y , magnetizations m_x, m_y and q and $|m|^2$ used for this analysis are computed from thermalized data produced using Monte Carlo simulations with the parallel tempering algorithm. For each case, we display (i) the comparison of the whole range of sorted original and inferred couplings, (ii) the comparison of inferred to original couplings to one single site and (iii) the sensitivity plots for true positive (fraction of original non-zero couplings inferred to be non-zero) against the number of predicted connections, yielding an insight into the topology of the graph.

3.1. Ordered couplings on complete graph

For the fully connected case the entire analysis is shown at $T = 0.5$, in the ferromagnetic phase. In Fig. 1 we display the comparison between the original (dotted/green lines) and the inferred (continuous/red and black lines) couplings sorted by magnitude in a system of $N = 64$ modes and $N(N - 1)/2 = 2016$ independent couplings. We consider three cases. On the left panel purely real, ferromagnetic $J_{ij} = J_{ji} = J$ couplings are plotted in a zero external magnetic field, $h = 0$, and for $h = 0.2$. To infer the values of J_{ij} we used Eq. (51) that fairly predicts the initial couplings even though the equations used are of the general case, i.e., complex Hermitian J 's that can take any value. Using, instead, Eq. (29) or Eq. (33), focused on the specific cases of purely real couplings and zero-field, no difference is appreciated down to the third digit.

In the mid and right panels, we plot real and imaginary inferred J 's with zero fields and for $h_R = 0.4, h_I = 0.2$. The quality of the prediction is comparable with the purely

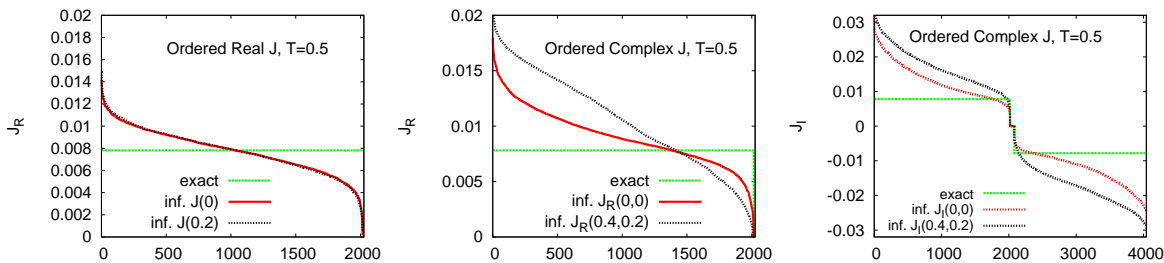


Figure 1: Sensitivity plot of the sorted inferred interaction couplings in the complete graph at $T = 0.5$ for an ordered system of $N = 64$ variables. Left: Ordered, only real J for $h = 0, 0.2$. Right: J_R and J_I for $\mathbf{h} = (h_R, h_I) = (0, 0)$ and for $\mathbf{h} = (0.4, 0.2)$.

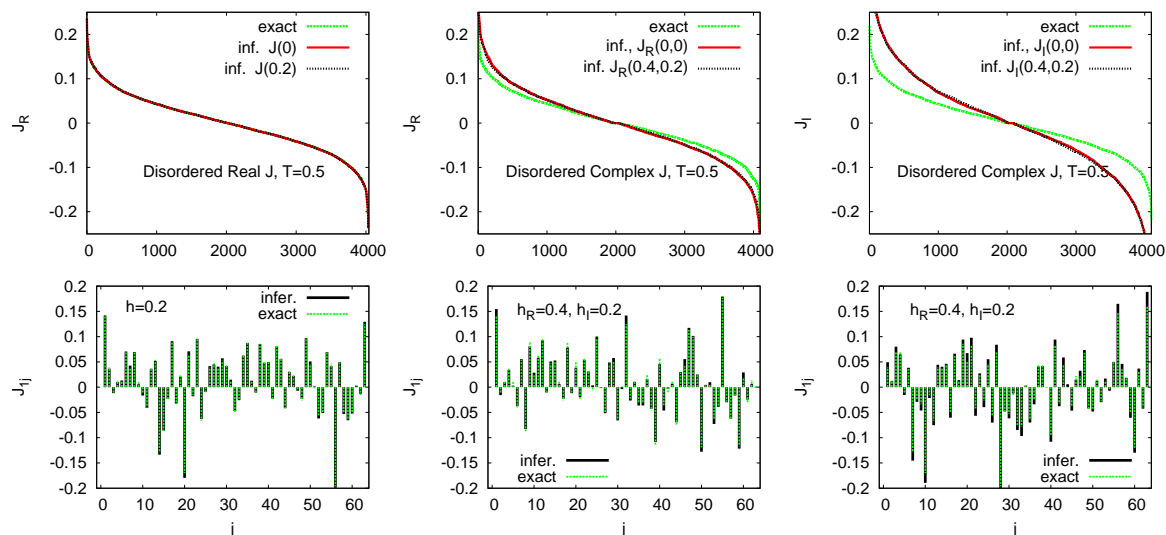


Figure 2: Sensitivity plot of the sorted inferred interaction couplings in the complete graph with $N = 64$ and quenched disorder at $T = 0.5$, in the spin-glass phase. Left: Purely real valued J for $h = 0, 0.2$. Right: Real and imaginary parts of the complex disordered couplings, J_R and J_I for $\mathbf{h} = (h_R, h_I) = (0.4, 0.2)$. Bottom panels: original and inferred couplings to a single site.

real case.

3.2. Disordered couplings on complete graph

We, then, inferred couplings from correlation functions and magnetizations generated in a system of $N = 64$ spins where J_R and J_I 's are originally generated by means of a Gaussian random distribution of mean zero and variance one. In the left panels (top and bottom) of Fig. 2 the case of purely real couplings is exposed, both in $h = 0$ and $h = 0.2$. No difference is appreciated between these two cases and the magnitudes of both are about the magnitude of the original couplings. As detailed in the bottom panel for couplings to a specific site, inferred J 's faithfully predict sign and magnitude of the original ones. The center and right panels display the behavior of real and imaginary part of a system with complex couplings both in absence and presence of external fields. Again, the presence of external fields do not alter the inference predictions and signs and magnitude of original couplings are correctly predicted.

3.3. Ordered couplings on sparse random graph

Next, we show the analysis for the case where the J matrix is diluted, though the formalism developed in this work is rigorous for fully connected systems and not for sparsely connected ER graphs. The connectivity probability is randomly distributed according to Eq. (54) with average connectivity $c = 6$. Data shown are for $N = 256$ spins at temperature $T = 2.5 > T_c \sim 1.95$ for the systems with complex Hermitian

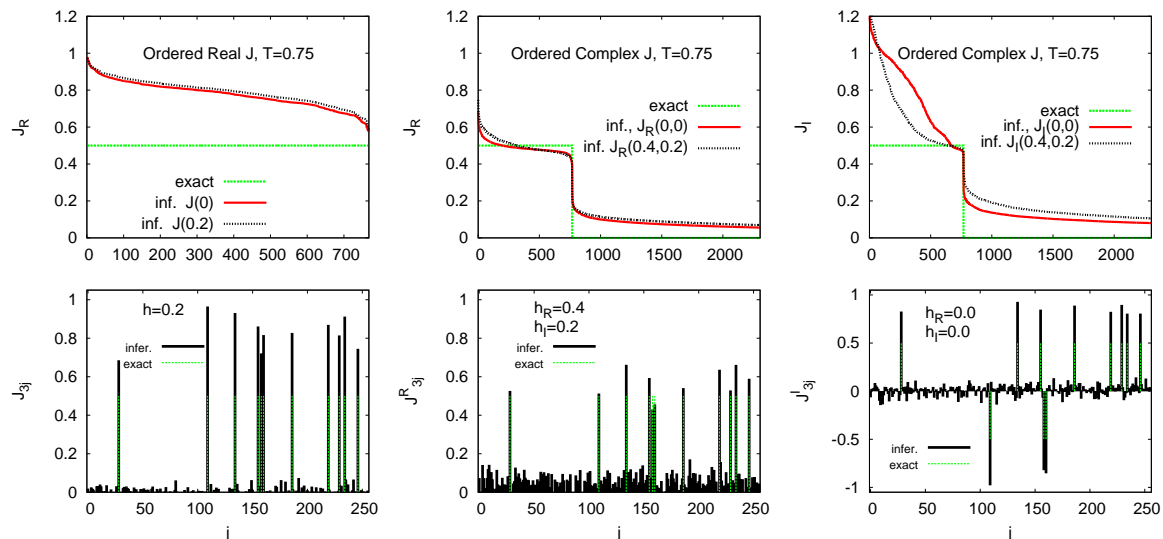


Figure 3: Sensitivity plot for the inferred couplings of an original random ER graph of $N = 256$ nodes with fixed deterministic values of J at $T = 0.75$. Left: Real valued J 's for the largest entries (first $N c/2$ elements, $c = 6$). Right: Real and imaginary part of complex couplings (first $3/2N c$ entries). Bottom panels: original and inferred couplings to a single site.

couplings, cf. Eq. (38) and $T = 0.75$ (here $T_c = 2.958$) for systems with purely real couplings, given by Eq. (1).

In Fig. 3 we display the comparison of the inferred and the original J 's by means of Eq. (51). In the left panels original couplings are all real and, when non-zero, all equal to each other. Each site is connected to a finite, N -independent, number of others, $c = 6$ in the average. The analysis gives correct indication for non-zero J_R 's both in absence and presence of external fields. However, our method always provide non-zero (though small) predictions for all couplings. Indeed, the true positive plots, cf. Fig. 4, decay down to zero only gradually, not sharply, quantifying the wrong predictions. Even though all non-zero elements of the matrix have been predicted correctly, for every zero element the formalism does not predict exact zero, bringing down the score of true positive.

The same situation arises for complex couplings, where rather good estimates of non-zero J^R and J^I entries is provided, including a sharp decrease of the value of the inferred couplings at the sorted coupling $N c/2$, cf. top panels in Fig. 3. This is, though, contrasted by the rather poor estimate of zero couplings. As confirmed by the true positive plots in Fig. 4, the right panels of Fig. 3 show that zero couplings, i. e., those beyond the $N c/2$ -th coupling, are inferred to acquire a non-zero value. Zero original couplings are not reproduced at all in the sparse case.

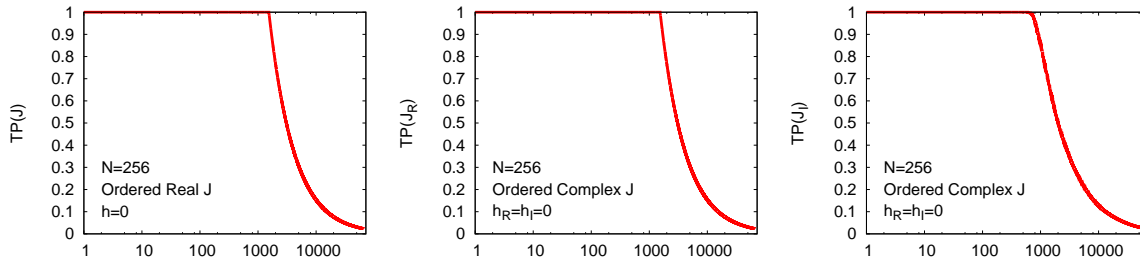


Figure 4: True positive plots for the ER sparse random graph with average connectivity $c = 6$, size $N = 256$ and with deterministic couplings $J = 1$.

3.4. Disordered couplings on sparse random graph

The inference maintains the same quality also in the case of random values of the couplings. In Fig. 5, left panels, we display the case of a ER random graph whose couplings have Gaussian distributed real values, with average zero and variance equal to one. The top figure in the sensitivity plot for the first $N c/2$ couplings, with and without external field, compared to the original disordered coupling values. The bottom panel show the comparison between original and inferred couplings to the graph node 3, to exemplify that: (i) all original non-zero couplings are well reproduced and discriminated in the inference procedure and (ii) all inferred couplings are non zero, also those corresponding to missing original couplings, though the latter acquire a rather small value in comparison to the inferred true links. The same analysis is illustrated in the mid and right panels of Fig. 5 for the real and imaginary part of a system with Hermitian couplings. In the sensitivity plot the first and last $3 N c/2$ couplings are reported and compared to the original ones, signaling that the inference quality is very good, though non-zero couplings are inferred to have a small non-zero value. In the bottom panels couplings to one node are displayed. This is confirmed in Fig. 6 where the true positive curve is shown to decrease sharply after the last non-zero coupling but still is non-zero for all J_{ij} matrix entries in all considered cases.

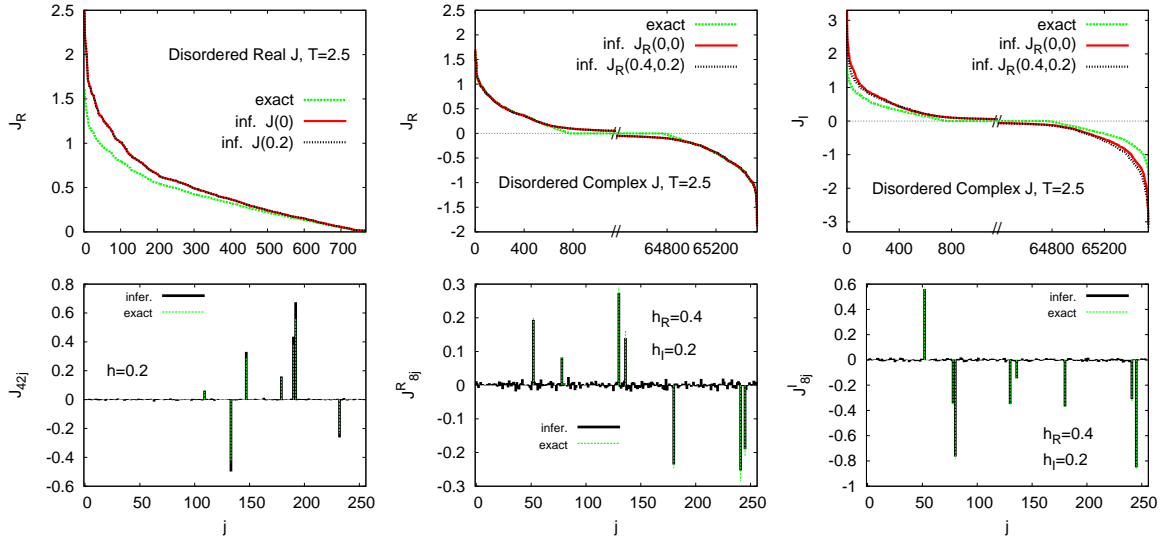


Figure 5: Sensitivity plot for the inferred couplings of an original random ER graph with Gaussian distributed random couplings (zero mean, unitary variance) at $T = 2.5$ and with $N = 256$. Left: Real valued J 's for the largest entries (first $N c/2$ elements). Right: Real and imaginary part of complex couplings (first and last $3/4N c$ entries). Bottom panels: original and inferred couplings to a single site.

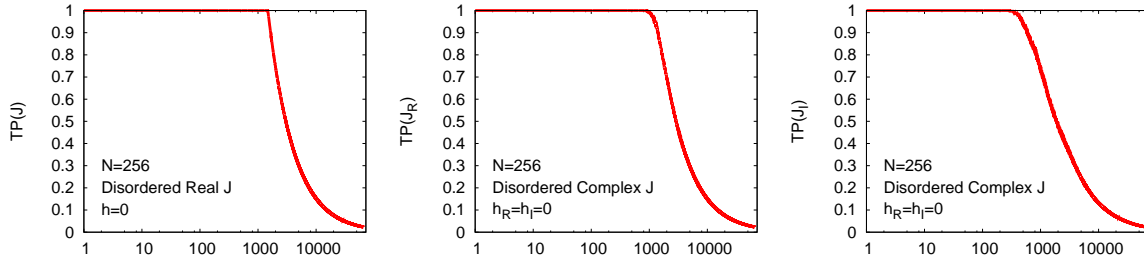


Figure 6: True positive plots for the ER sparse random graph with average connectivity $c = 6$, size $N = 256$ and with Gaussian random distributed couplings (zero mean, unit variance). Left: True positive of a system with purely real couplings and zero external field. Mid and Right: True positive of the real and imaginary parts of the couplings in a system with zero field.

4. Small data size behavior

In this part, we show how the quality of inference is deteriorated as the number of measurements composing the data set used to calculate correlations decreases. In the main figure 7, the entire sorted J matrix is shown and in the inset the absolute value of the first 2000 elements are shown. We see that the sensitivity plot remains the qualitatively the same for all data sets, but the transition from non-zero to zero couplings becomes sharper and sharper as the data size increases, yielding evidence for an underlying sparse graph.

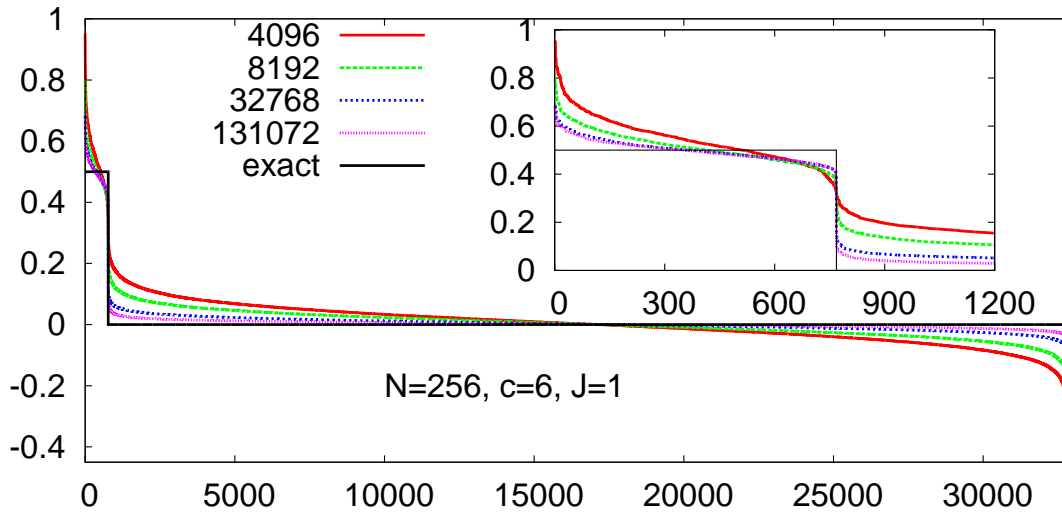


Figure 7: Sensitivity plot of data generated from an ER graph of $N = 256$ sites and mean connectivity $c = 6$ with real ordered couplings and no field. The behavior of the original network is marked as a full black step curve. Correlation functions averaged over, respectively, 4096, 8192, 32768 and 131072 data from Monte Carlo simulations are considered. In the inset a detail of the absolute values of the bonds around the last non-zero original coupling ($N c/2 = 768$) is provided.

5. Conclusions

In the present paper we have derived an inference procedure to determine the coupling constants of pairwise interacting systems with continuous XY spins, complex interactions and complex external fields.

For testing the analytic inference approach we have applied it to data numerically generated by means of Monte Carlo simulations at equilibrium and we have compared the inferred values of the coupling constants to the ones of the simulated system. We considered models with disorder in the coupling values and models with disorder in the coupling connectivity, studying both complete and sparse random graphs with both deterministic and quenched disordered couplings. The inferred couplings turn out to reproduce original ones in an excellent way in fully connected models, that is, under the conditions at the ground of the theoretical derivation of inference formulas Eqs. (29, 51, 52). Also when applied to sparse random graphs, though, the quality of the inference is of a high standard. The only problem arises in the wrong representation for missing links that acquire always non-zero value in the inference procedure. Their values, actually, decrease with increasing data size, but do not reach zero even for very large data sizes, cf. Fig. 7. Else said, the true positive curve is always non-zero for all couplings. The value of false positive inferred couplings turns out, though, to be systematically much smaller than the value of true positive bonds, with a sharp quantitative distinction between the two.

In the field of random photonics, the reported method to quantitatively infer coupling constants from experimental data would allow to obtain estimates of the effective damping interaction between localized modes in a random medium mediated by radiative modes [18, 19, 20] in an open cavity, to extrapolate the magnitude of the optical-response-modulated spatial overlap between those modes [21] and, eventually to obtain information about their localizations. Further on, the inference method for XY pairwise models can be applied to the optimization of the output signal from complex random media [23, 24], including disordered optical fibers, by inferring the elements of the transmission matrix.

Further investigation on inference of waves can include alternative probes of the linear problem here reported by means of other inference methods such as pseudo-likelihood. Most interesting is the generalization to nonlinear problems, allowing for the reconstruction of the properties of light modes in both ordered and random lasers, both in the continuous and in the pulsed regime [27, 47].

Acknowledgments

We thank Marco Zamparo and Riccardo Zecchina for interesting discussions on the problem. The research leading to these results has received funding from the Italian Ministry of Education, University and Research under the Basic Research Investigation Fund (FIRB/2008) program/CINECA grant code RBFR08M3P4 and under the PRIN2010 program, grant code 2010HXAW77-008 and from the People Programme (Marie Curie Actions) of the European Union's Seventh Framework Programme FP7/2007-2013/ under REA grant agreement n 290038, NETADIS project.

Bibliography

- [1] Stanley H E 1968 *Phys. Rev. Lett.* **20** 589
- [2] Vaks V G and Larkin A I 1966 *Soviet Phys. - JETP* **22** 678
- [3] Brézin E 1982 *J. Phys. (France)* **43** 15
- [4] Kosterlitz J and Thouless D 1972 *J.Phys.C* **5** L124–L126
- [5] Kosterlitz J M and Thouless D J 1973 *J. Phys. C* **6** 1181–1203
- [6] Kosterlitz J and Thouless D 1972 *J.Phys.C* **7** 1046
- [7] Bokil H S and Young A P 1996 *J. Phys. A* **29** L89
- [8] Kawamura H 2010 *J. Phys. Soc. Japan* **79** 011007
- [9] Alba V, Pelissetto A and Vicari E 2010 *J. Stat. Mech.* **2010** P03006
- [10] Obuchi T and Kawamura H 2013 *Phys. Rev. B* **87**(17) 174438
- [11] Cassi D 1992 *Phys. Rev. Lett.* **68** 3631
- [12] Burioni R, Cassi D and Vezzani A 1999 *Phys. Rev. E* **60** 1500
- [13] Ibáñez Berganza M and Leuzzi L 2013 *Phys. Rev. B* **88** 144104
- [14] Cardy J 1996 *Scaling and Renormalization in Statistical Physics* (Cambridge: Cambridge University Press)
- [15] Kuramoto Y 1975 *Lect. N. Phys.* **39** 420–422
- [16] Acebrón J A, Bonilla L L, Pérez Vicente C J, Ritort F and Spigler R 2005 *Rev. Mod. Phys.* **77** 137
- [17] Gupta S, Campa A and Ruffo S 2014 *J. Stat. Mech.* R08001

- [18] Hackenbroich G, Viviescas C and Haake F 2002 *Phys. Rev. Lett.* **89** 083902
- [19] Viviescas C and Hackenbroich G 2003 *Phys. Rev. A* **67** 013805
- [20] Hackenbroich G, Viviescas C and Haake F 2003 *Phys. Rev. A* **68** 063805
- [21] Antenucci F, Conti C, Crisanti A and Leuzzi L 2015 *Phys. Rev. Lett.* **114** xxx
- [22] Antenucci F, Crisanti A and Leuzzi L 2014 (*Preprint arXiv:1412.8706*)
- [23] Popoff S M, Lerosey G, Carminati R, Fink M, Boccara A C and Gigan S 2010 *Phys. Rev. Lett.* **104** 100601
- [24] Akbulut D, Huisman T J, van Putten E G, Vos W L and Mosk A P 2011 *Opt. Expr.* **19** 4017
- [25] Nobre F D, Sherrington D and Young A P 1989 *J. Phys. A* **22** 2835
- [26] Ilker E and Nihat Berker A 2013 *Phys. Rev. E* **87** 032124
- [27] Marruzzo A and Leuzzi L 2014 (*Preprint arXiv:1411.4674*)
- [28] Lupo C and Ricci-Tersenghi F 2014 in preparation
- [29] Kappen H J and Rodríguez F B 1998 *Neural Comp.* **10** 1137
- [30] Tanaka T 1998 *Phys. Rev. E* **58** 2302
- [31] Mézard M and Montanari A 2009 *Information, Physics, and Computation* (Oxford University Press)
- [32] Sessak V and Monasson R 2009 *J. Phys. A* **42** 055001
- [33] Roudi Y, Hertz J and Aurell E 2009 *Front. Comp. Neuros.* **3** 22
- [34] Morcos F, Pagnani A, Lunt B, Bertolino A, Marks D S, Sander C, Zecchina R, Onuchic J N, Hwa T and Weigt M 2011 *Poc. Natl. Acad. Sci.* **108** E1293–E1301
- [35] Marks D S, Colwell L J, Sheridan R, Hopf T A, Pagnani A, Zecchina R and Sander C 2011 *PLoS ONE* **6** e28766
- [36] Baldassi C, Zamparo M, Feinauer C, Procaccini A, Zecchina R, Weigt M and Pagnani A 2014 *PLoS ONE* **9** e92721
- [37] Schneidman E, Berry M J, Segev R and Bialek W 2006 *Nature* **440** 1007–1012
- [38] Garel T, Iori G and Orland H 1996 *Phys. Rev. B* **53**(6) R2941–R2944
- [39] Murray Sargent III, Marlan O'Scullly and Willis E Lamb 1978 *Laser Physics* (Addison Wesley Publishing Company)
- [40] Gordon A and Fischer B 2002 *Phys. Rev. Lett.* **89** 103901
- [41] Angelani L, Conti C, Ruocco G and Zamponi F 2006 *Phys. Rev. Lett.* **96** 065702
- [42] Fox A and LI T 1968 *IEEE J. Quant. Elec.* **4** 460
- [43] Wiersma D S 2008 *Nature Physics* **4** 359
- [44] Ghofraniha N, Viola I, Di Maria F, Barbarella G, Gigli G, Leuzzi L and Conti C 2014 *Nat. Commun.* **6** 6058
- [45] Eremeev V, Skipetrov S E and Orszag M 2011 *Phys. Rev. A* **84** 023816
- [46] Conti C and Leuzzi L 2011 *Phys. Rev. B* **83** 134204
- [47] Antenucci F, Ibáñez Berganza M and Leuzzi L 2014 (*Preprint arXiv:1409.6345*)
- [48] Newman M E J 2003 *SIAM Rev.* **45** 167256